



Available online at www.sciencedirect.com

ScienceDirect

Energy Procedia 124 (2017) 384-391



7th International Conference on Silicon Photovoltaic, SiliconPV 2017

Analysis of contact recombination at rear local back surface field via boron laser doping and screen-printed aluminum metallization on p-type PERC solar cells

Yuka Tomizawa^a*, Yoshinori Ikeda^a*, Haruhiko Itoh^a, Takashi Shiro^a, Jochen Loffler^b, Petra Manshanden^b, Ingrid Romijn^b

^aTeijin Limited, 4-3-2, Asahigaoka, Hino-shi, Tokyo, 191-8512, Japan ^bECN Solar Energy, Westerduinweg 3, 1755 LE Petten P.O.Box 1, 1755 ZG Petten, Netherlands

Abstract

The passivated emitter and rear cell (PERC) has entered the solar cell market, and it is expected that the amount of PERC production will increase yearly in the future. Improvements in the cell efficiency have a great influence on reducing the cost of power generation. In this study, we focused on the loss of the back surface field (BSF) at the rear side of a PERC, fabricated PERCs having a local BSF including boron diffused by boron laser doping (B-LD), and evaluated this effect. The results from an analysis using scanning electron microscopy (SEM) indicated that the thickness of the BSF fabricated with B-LD was thicker than that of the BSF fabricated without B-LD. The average value of the saturation current density of the metallized area (including BSF) $J_{0,\, \text{contact}}$ was 554 fA/cm² in the PERCs fabricated with B-LD and a dedicated Al paste, and the lowest value achieved was approximately 300 fA/cm². The number of Kirkendall voids for the PERCs fabricated with B-LD decreased in comparison with the PERCs fabricated without B-LD. The PERCs fabricated with B-LD exhibited reduced rear-side recombination.

© 2017 The Authors. Published by Elsevier Ltd.

Peer review by the scientific conference committee of SiliconPV 2017 under responsibility of PSE AG.

Keywords: Si nanoparticle; laser doping; local back surface field

^{*} Corresponding author. Tel.: +81-42-586-8512; fax: +81-42-587-5510. *E-mail address*: y.tomizawa@teijin.co.jp, yos.ikeda@teijin.co.jp

1. Introduction

Nowadays, the application of a passivated emitter and rear cell (PERC) is attractive for high-efficiency solar cells, and a cell efficiency greater than 22% has been realized at the pilot level [1-4]. The cell properties of a PERC have been improved using various approaches, but characteristic improvements in a PERCs are still demanded. It has been reported by simulation of the loss in the cell properties that the loss in the rear-side local back surface field (BSF) is large [5-8]. For the development of the rear-side local BSF, an Al-alloyed BSF layer is commonly used in a PERC, and there are few examples that have attempted to use this new concept. It has been reported that the saturation current density of the metallized area (including the BSF) $J_{0, \, \text{contact}}$ can be reduced by using an Al paste containing a B additive [9, 10] because it improves the BSF effect owing to the high dopant concentration due to the codiffusion of B and Al in the Al–Si liquid phase above the eutectic temperature (577 °C). However, it is well known that a large amount of B additives in the Al paste deteriorate the electrical properties of the Al electrode [10]. Another issue associated with PERCs is Kirkendall voids, and the composition of the Al paste and the firing conditions have been studied to prevent Kirkendall voids in PERCs [11, 12].

We developed a B laser doping (B-LD) technique with B-doped silicon nanoparticles (Si NPs) to achieve an improvement in the efficiency of PERCs by having a local BSF including B [13]. The local BSF with B improved the internal quantum efficiency (IQE) in the long-wavelength region, which means that the back side of the cell increased its efficiency, particularly the open-circuit voltage V_{oc} and fill factor, in comparison with a cell without B-doped Si NPs. We reported that the local BSF layer of a PERC that exhibited a high V_{oc} and high cell efficiency included a B content greater than 0.9 wt%. Moreover, we showed that the B in the local BSF layer influenced the diffusion of Al and enhanced the local BSF effect [14]. It was observed that B-LD combined with screen-printed Al metallization leads to a thicker local BSF and a reduction in the number of voids [15, 16].

In this study, we evaluated PERCs fabricated with and without B-LD to determine $J_{0, \, contact}$ and the number of Kirkendall voids to clarify the effects of B in detail. The local BSF and Kirkendall voids in each cell were observed using scanning electron microscopy (SEM), and $J_{0, \, contact}$ was determined from the changes in the saturation current density J_0 with different electrode contact area ratios.

2. Experiments

A schematic of the B-LD and screen-printed Al metallization procedure is shown in Fig. 1. The local BSF layer of the PERCs using B-LD was fabricated by irradiating a substrate printed with a B-doped Si NP paste with a green laser and subsequent metallization using an Al paste. Figure 2 shows a schematic of the cross section of the PERCs. The B-LD technique with the B-doped Si NP paste was used for the back side of the cells. Figure 3 shows a magnified view of the local BSF of the area enclosed in the yellow square in Fig. 2. Two types of cells with different BSF layers formed by B-LD and only the Al paste were fabricated. The BSF formed by B-LD has a B/Al local BSF layer, and the BSF formed by the Al paste has an Al local BSF layer. Al dissolved as the temperature of the cofiring process increased, and a reaction between Al and Si started. B diffused with Al and Si during the cofiring process, and the B/Al local BSF layer formed as shown in Fig. 4 [14].

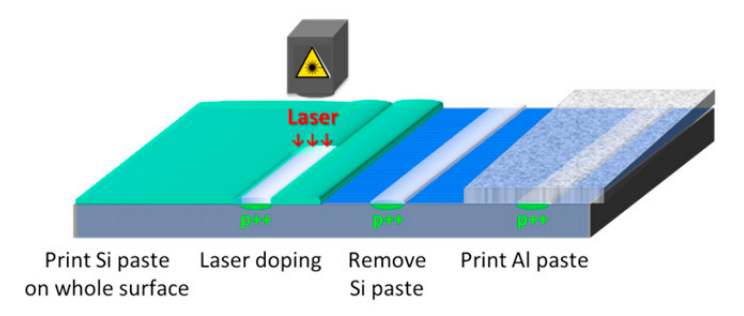


Fig. 1. Schematic of B-LD and screen-printed aluminum metallization.

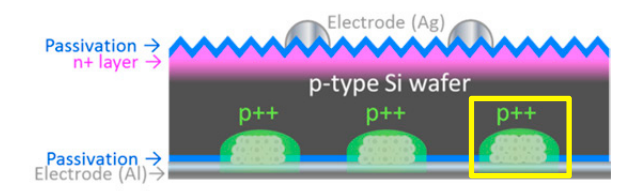


Fig. 2. Schematic of the cross section of a PERC.

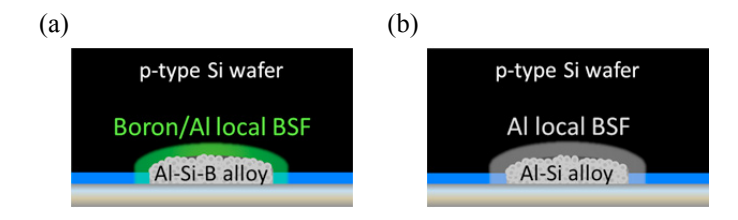


Fig. 3. Comparison of the BSF layers formed by (a) B-LD and (b) Al paste.

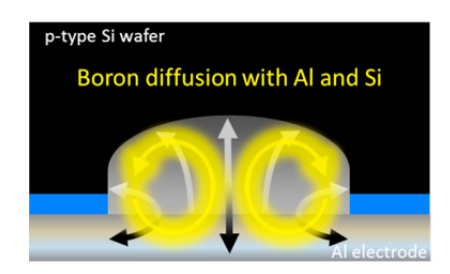


Fig. 4. Mechanism by which the B/Al local BSF layer is formed. The yellow arrows show the diffusion of B.

A conventional PERC that did not use the B-doped Si NP paste was prepared as a reference cell. All PERCs had dimensions of $50 \times 50 \text{ mm}^2$ and were processed on p-type Czochralski-grown Si wafers with a thickness of $180 \pm 30 \, \mu\text{m}$. An alkali texturing process was performed after cleaning. The sheet resistance after P emitter diffusion was $70-80 \, \Omega/\text{sq}$. A passivation stack consisting of AlO_x deposited by atomic layer deposition (ALD) and SiN_x deposited by plasma-enhanced chemical vapor deposition (PECVD) was applied on the rear side of the cells. The front of the cells is passivated by PECVD SiN_x. Boron was locally diffused into the rear side using laser doping with the B-doped Si NP paste as the source. The Si NP paste was printed onto the full rear Al₂O₃/SiN_x passivation layer area and dried at 200 °C for 10 min. The dried Si NP film thickness was approximately 2.0 μ m. A 532 nm pulsed laser (frequency: 150 kHz, pulse width: 20 ns, laser fluence: 2.0 J/cm²) was used for laser doping. The overlap of the laser was changed in the cell using B-LD to investigate the most suitable condition (75%, 90%, 95%). The sheet resistance of the B-LD area decreased to 35 Ω/sq for a laser overlap of 90%, as measured using the four-point probe method on test samples with larger laser doped areas of $1.5 \times 1.5 \, \text{cm}^2$. To measure $J_{0, \, \text{contact}}$ with reasonable error margins, a large range of electrode contact area ratios and a high absolute electrode contact area ratio are preferred. Therefore, B-LD was carried out using a 40 μ m line width for patterns with three different pitches: 0.3, 0.6, and 1.0 mm. After B-LD, the Si NP residue was removed by immersion in a 1.0 wt% aqueous KOH solution heated to 80

°C. Figure 5 shows SEM images of the surfaces at laser opening and the B-LD area with the B-doped Si NP paste after KOH treatment. These surfaces are smooth and almost the same roughness; it is thought that these surfaces had few significant effects on the reactivity with the Al paste during cofiring. Al and Ag pastes were screen-printed onto the rear and front, respectively, and cofired. The most suitable cofiring condition was used depending on the laser doping condition. The rear contact line width after cofiring was approximately 100 μm, resulting in electrode contact area ratios of 30.9%, 15.9%, and 9.4% for the three B-LD pitches. Two types of Al pastes were compared: a conventional Al paste and a dedicated Al paste for the PERC.

The completed solar cells were characterized by current-voltage (I–V) measurements. The total saturation current density $J_{0, \text{cell}}$ for all cells was determined from the short-circuit current density J_{sc} and V_{oc} using the one-diode equation assuming a diode ideality factor of n=1. This assumption is based on the fact that contact recombination can best be described with n=1 recombination, while experimental cells have n values around 1.1. $J_{0, \text{contact}}$ was determined from the changes in $J_{0, \text{cell}}$ with different electrode contact area ratios (depending on the pitch/number of laser lines) [18]. In practice, the values of $J_{0, \text{contact}} - J_{0, \text{pass}}$ deduced from the analysis do not allow the determination of the saturation current density of the passivated area $J_{0, \text{pass}}$ with a reasonable error margin, as $J_{0, \text{cont}}$ is much larger than $J_{0, \text{pass}}$ and has a significant error margin. Therefore, $J_{0, \text{pass}}$ was conservatively assumed to be 50 fA/cm² in order to obtain an upper boundary for $J_{0, \text{contact}}$. SEM was used to observe the cross sections of the B-LD areas on the rear sides of the cells to measure the dimensions of the local BSF and the percentage of voids.

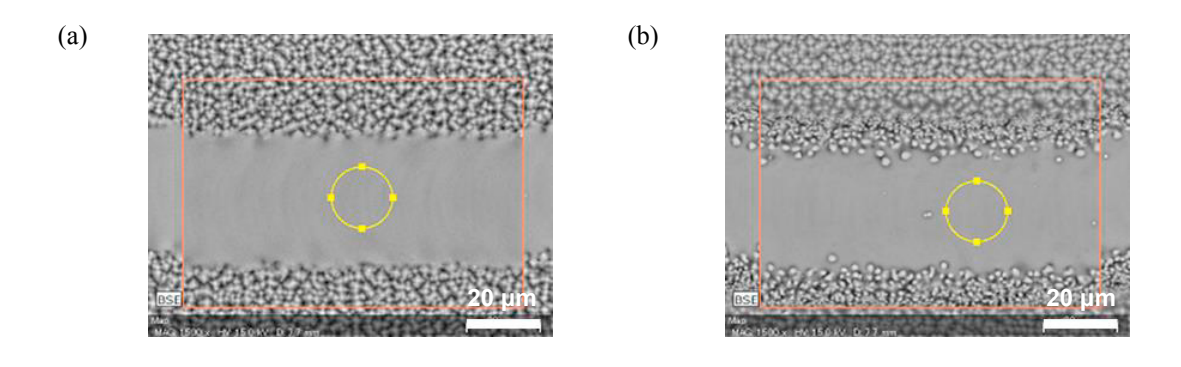


Fig. 5. SEM images of the surfaces at the line-patterned areas of PERCs fabricated (a) with and (b) without B-LD.

3. Results and discussion

The local BSF layers observed by SEM are shown in Fig. 6. The thickness of the local BSF layer was determined as the average of ten measurements with SEM. The thicknesses of the local BSF layers fabricated with and without B-LD were 3.8 and 2.4 μ m, respectively. Thus, a thicker BSF layer formed in the PERC contacts using B-LD compared with the conventional PERC. The contact width of the Al–Si–(B) alloy and Al paste was about 100 μ m. This means that the contact width spread by cofiring because the line width of the laser was 40 μ m. Remarkably, a high B concentration in the local BSF layer was observed for the PERCs fabricated using B-LD, and in a previous paper [14], the B/Al ratio from secondary ion mass spectroscopy (SIMS) measurements was calculated to be 0.9 wt% or higher [13, 14]. It was reported that the PERC fabricated using B-LD achieved a higher V_{oc} and fill factor (FF), which can be explained by the thicker BSF layer and the reduction in the number of voids.

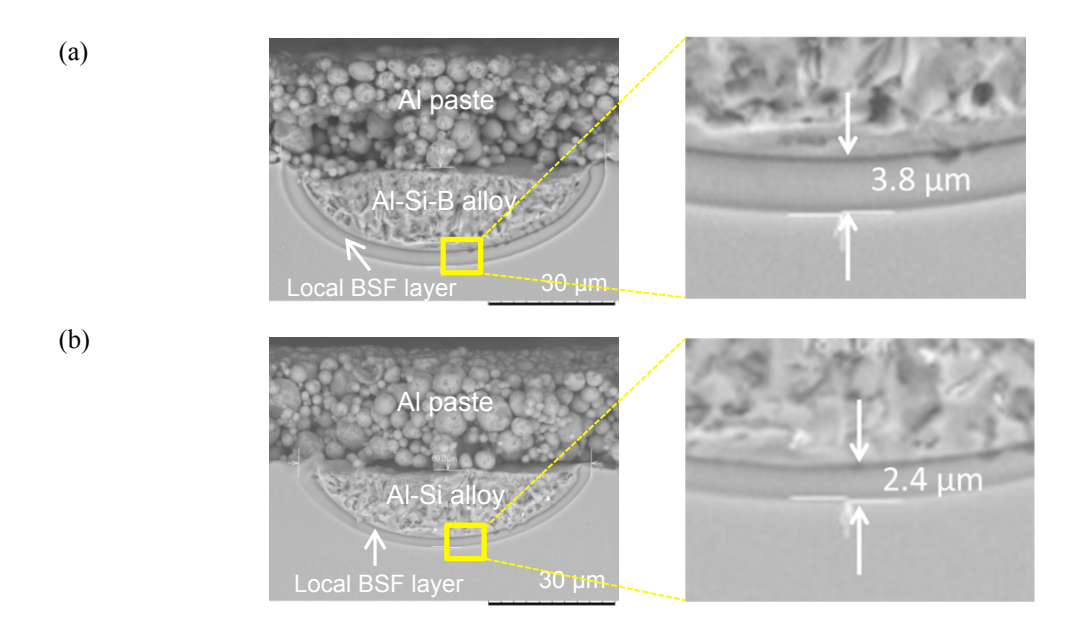


Fig. 6. SEM images of the local BSFs of PERCs fabricated (a) with and (b) without B-LD. The right figures are magnifications of the left figures (the areas enclosed in yellow squares).

 $J_{0,\,\,{\rm contact}}$ was evaluated to determine the effect of a thick BSF layer in the PERCs fabricated with B-LD. Figure 7 shows a comparison of $J_{0,\,\,{\rm contact}}$ for the PERC sample fabricated with and without B-LD. Figures 7(a) and (b) show the results obtained for the PERC contacts utilizing the conventional and dedicated Al pastes, respectively. The average values of $J_{0,\,\,{\rm contact}}$ for the PERC contacts fabricated without and with B-LD and the conventional Al paste were 3670 and 980 fA/cm², respectively. $J_{0,\,\,{\rm contact}}$ for the cell fabricated with B-LD and the conventional Al paste decreased in comparison with that of the cell without B-LD. Similarly, when using the dedicated Al paste for PERC, $J_{0,\,\,{\rm contact}}$ showed a tendency to decrease. The average values of $J_{0,\,\,{\rm contact}}$ from the PERCs fabricated without and with B-LD and the dedicated Al paste were 891 and 554 fA/cm², respectively. $J_{0,\,\,{\rm contact}}$ for the PERC samples fabricated with B-LD and the dedicated Al paste was smaller than that fabricated without B-LD and both pastes, and the lowest value achieved was approximately 300 fA/cm². $J_{0,\,\,{\rm contact}}$ was rather low for a laser overlap of 90%. This result indicates that B-LD enhances the local BSF effect by suppressing rear-side recombination and reduces $J_{0,\,\,{\rm contact}}$ of the PERCs.

Figure 8 shows the percentage of Kirkendall voids for these cells. The percentage of Kirkendall voids in the PERCs fabricated with B-LD and the dedicated Al paste was less than 10% under the cofiring temperature

conditions. On the other hand, the percentage of Kirkendall voids for the PERCs fabricated without B-LD was greater than 20%. Normally, the Si base material diffuses into the Al paste and vice versa, and the difference in the diffusivities causes the Kirkendall effect. Subsequently, voids are formed, and the cell performance decreases because the contact resistance of the electrode and Si base material increases [17]. These results indicate that the local BSF layer fabricated with B-LD improves the contact resistance by controlling the generation of voids and the cell properties improve because of the thicker local BSF [15, 16]. B-LD reduces the occurrence of Kirkendall voids, and it is thought that the interaction between the Al paste and the Si surface with B formed from the B-doped Si NP paste might be different compared to that without B [15].

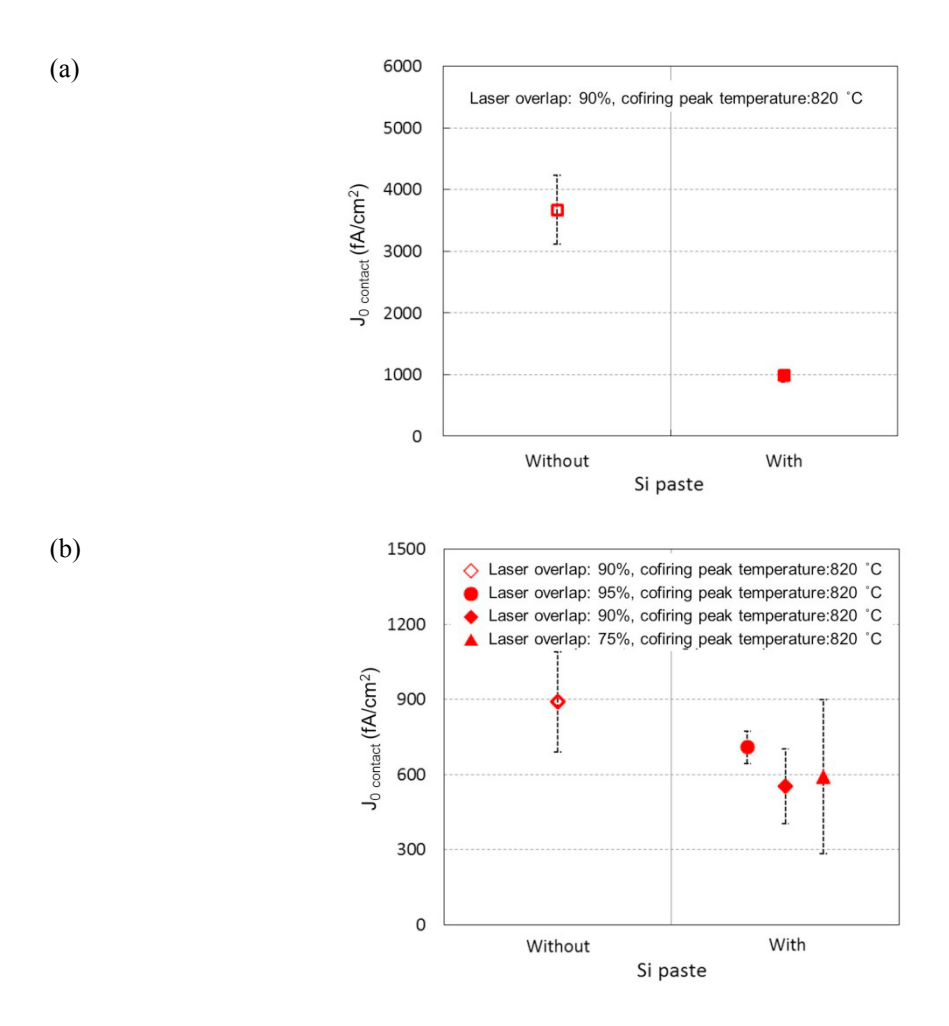


Fig. 7. Saturation current density of the metallized area $J_{0, contact}$ for PERCs fabricated with and without B-LD from the B-doped Si NP paste, metallized by two different Al pastes: (a) conventional and (b) dedicated Al pastes for the PERCs. Error bars reflect the standard error of the linear fit of J_0 versus the metal fraction.

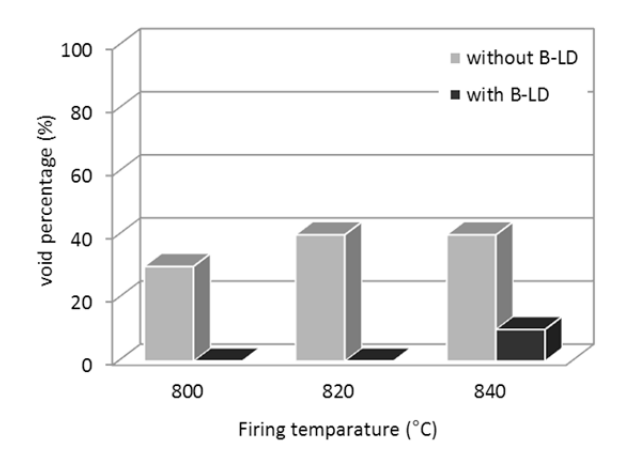


Fig. 8. Percentage of Kirkendall voids in PERCs fabricated with and without B-LD.

4. Conclusion

A PERC fabricated with B-LD and screen-printed Al metallization was developed and studied to increase the cell efficiency by improving the rear-side local BSF. A B-doped Si NP paste was used as a B source. In the PERCs fabricated with B-LD, an obviously thicker BSF layer was achieved compared to that for a conventional PERC. $J_{0, \text{contact}}$ for the PERC contacts fabricated using the dedicated Al paste was smaller than that for the PERC samples fabricated using conventional Al. $J_{0, \text{contact}}$ of the PERCs fabricated with B-LD was low in comparison with that of the conventional PERC, and the minimum value was approximately 300 fA/cm². Moreover, the number of Kirkendall voids was reduced and could be controlled to less than 10%. The PERCs fabricated with B-LD exhibited an enhanced local BSF effect due to the suppression of rear-side recombination and a reduction in $J_{0, \text{contact}}$. The PERCs fabricated with B-LD exhibit lower Kirkendall void formation, which has been reported to lead to a decreased contact resistance. These results are expected to enable a higher V_{oc} and FF and therefore also improve the solar cell efficiency.

References

- [1] Blankers AW, Wang A, Miline AM, Zhao J, Green MA. 22.8% efficiency silicon solar cell. Appl Phys Lett 1989;55:1363-5.
- [2] Nekarda J, Lottspeich F, Wolf A, Preu R. Silicon solar cells using aluminum foil as rear side metallization reaching 21.0% efficiency. 25th European Photovoltaic Solar Energy Conference and Exhibition 2010:2211-4.
- [3] Green MA. The passivated emitter and rear cell (PERC): From concept to mass production. Sol Energy Mater Sol Cells 2015;143:190-7.
- [4] Dullweber T, Schmidt J. Industrial silicon solar cells applying the passivated emitter and rear cell (PERC) concept A review. IEEE J Photovolt 2016;6:1366-81.
- [5] Chen D, Deng W, Li H, Dong J, Ye F, Chen Y, Zhu H, Zhong M, Zhang Y, Feng Z, Verlinden PJ. Metallization of rear local point-contacts for industrial PERC solar cells. Proceedings of the 29th Europian Photovoltaic Solar Energy Conference and Exhibition 2014:1383-6.
- [6] Lauermann T, Fröhlich B, Hahn G, Terheiden B. Diffusion-based model of local Al back surface field formation for industrial passivated emitter and rear cell solar cells. Prog Photovolt Res Appl 2015;23:10-8.
- [7] Kranz C, Baumann U, B. Wolpensinger, Lottspeich F, Müller M, Palinginis P, Brendel R, Dullweber T. Void formation in screen-printed local aluminum contacts modelled by surface energy minimization. Sol Energy Mater Sol Cells 2016;158:11-8.
- [8] Deng W, Ye F, Xiong Z, Chen D, Guo W, Chen Y, Yang Y, Altermatt P, Feng Z, Verlinden PJ. Development of high-efficiency industrial p-type multi-crystalline PERC solar cells with efficiency greater than 21%. Energy Procedia 2016;92:721-9.
- [9] Rauer M, Schmiga C, Tuschinsky A, Glatthaar M, Glunz SW. Investigation of aluminum-boron doping profiles formed by coalloying from screen-printed pastes. Energy Procedia 2013;43:93-9.

- [10] Rauer M, Schmiga C, Glatthaar M, Glunz SW. Alloying from screen-printed aluminum pastes containing boron additives. IEEE J Photovolt 2013;3:206-11.
- [11] Dressler K, Kratt M, Voss PA, Ebert S, Herguth A, Hahn G. Influence of Al particle size and firing profile on void formation in rear local contacts of silicon solar cells. IEEE J Photovolt 2016;6:68-73.
- [12] Chen D, Deng W, Sheng J, Zhu H, Zhong M, Wang W, Ye F, Cai W, Feng Z, Zhang Y, Shen H, Verlinden PJ. Preventing the formation of voids in the rear local contact areas for industrial-type PERC solar cells. 28th European Photovoltaic Solar Energy Conference 2013:770-4.
- [13] Tomizawa Y, Imamura T, Soeda M, Ikeda Y, Shiro T. Laser doping of boron-doped Si paste for high efficiency silicon solar cells. Jpn J Appl Phys 2015;54:08KD06.
- [14] Ikeda Y, Tomizawa Y, Itoh H, Shiro T. Investigation of rear localized back surface field formed from boron laser doping and screen-printed aluminum paste in high-efficiency solar cells. Energy Procedia 2016;92:404-11.
- [15] Hong J, Xuan R, Huang H, Geng Q, Wang W. Si paste technology for high-efficiency solar cells. Sol Energy 2016;135:70-76.
- [16] Lin D, Abbott M, Lu PH, Xiao B, Hallam B, Tjahjono B, Wenham S. Incorporation of deep laser doping to form the rear localized back surface field in high efficiency solar cells. Sol Energy Mater Sol Cells 2014;130:83-90.
- [17] Horbelt R, Hahn G, Job R, Terheiden B. Void formation on PERC solar cells and their impact on the electrical cell parameters verified by luminescence and scanning acoustic microscope measurements. Energy Procedia 2015;84:47-55.
- [18] Fellmeth T, Born A, Kimmerle A, Clement F, Biro D, Preu R. Recombination at metal-emitter Interfaces of front contact technologies for highly efficient silicon solar cells. Energy Procedia 2011;8:115–21.